

# An Analytical Model of Optical Photon Transportation for Monolithic PET Detector

Juntang Zhuang, Peng Fan, Xinqiang Wang, Shi Wang, Yaqiang Liu, Zhaoxia Wu, Tianyu Ma\*

## I. INTRODUCTION

Monolithic scintillator detector have been shown to provide better energy resolution and sensitivity without degrading the spatial resolution [1]. But 3D position information extraction is much more complicated compared to discrete scintillator detector. 3D maximum likelihood-based approach and artificial neural network (ANN) method are widely used to extract position information [2]. However both methods need reference or training data sets measured from experiments. An analytical model to characterize the optical photon transportation process in the crystal can eliminate the measurement procedure and provide better positioning algorithm.

In this paper, a generic analytical model to characterize optical photon transportation in monolithic PET detector is proposed. This model calculates the expectation of light distribution on the detector, supposing a gamma interacts at a certain position in the crystal. Detector geometry and crystal surface treatment were also considered in the model. Accuracy of this model was validated by comparing calculated light distribution with that of GATE [3] Monte Carlo simulation for certain gamma interaction positions. Two factors were defined to measure the difference between model calculation and simulation. Correlation coefficient (CC) measures difference in shape of light distribution, and Normalized mean square error (NMSE) measures difference in value of light distribution. Excellent agreement is achieved in all cases, indicating the accuracy of this model.

## II. MODELS AND METHODS

### A. Description of the detector & crystal surface treatments

Figure 1 shows a schematic diagram of the monolithic LYSO detector module. The crystal size is  $20 \times 20 \times 20 \text{ mm}^3$ . All the crystal surfaces are polished. The bottom surface is coupled to an  $(8 \times 8)$  SiPM array as shown in Figure 1, the other surfaces are coated with reflecting films to reflect optical photons. For simplicity in calculation, coordinate origin is located at one vertex, SiPM is placed in  $z=0$  plane, and the whole scintillator is located in the 1<sup>st</sup> octant, so  $x$ ,  $y$  and  $z$  coordinates of the crystal are positive. The yellow point represents an interaction position of a gamma photon within scintillator.

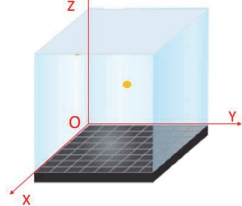


Fig.1. Schematic diagram of the simple detector module

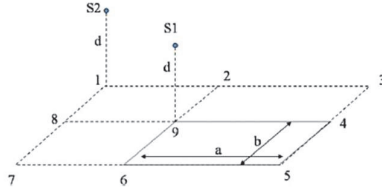


Fig.2. The relative position of point sources at S1 and S2, positioned at a distance  $d$  above a rectangular detector

Table 1 shows three commonly used crystal surface treatments studied in this work. Surfaces of crystal are polished, optical photons are absorbed in black film, and go through diffuse reflection in diffuse film. Between crystal surface and reflection film is a thin layer of silicone grease of constant refractive index.

In this model, only photon transportation within crystal is considered, and modeling about properties of SiPM and electronic noise are beyond the scope of this work.

Table 1. Three different crystal surface treatments used in the simulation

Crystal surface type	Crystal surface reflection type	Reflecting film type
BS	specular	black
SS	specular	specular
DS	specular	diffuse

### B. Optical photon transportation model

#### 1. Solid angle calculation

The number of optical photons directly reaching bottom surface is determined by solid angle subtended by that SiPM pixel seen from point source, as shown in Figure 2. For a point located at top of a vertex of a rectangle ( $a \times b$ ), its height is  $d$ , the solid angle of the rectangle seen from S1 is

$$\Omega = \arctan\left(\frac{ab}{d\sqrt{a^2 + b^2 + c^2}}\right) \quad (1)$$

If projection of source is outside the pixel, as S2 in figure 2, the solid angle is a linear combination of four other solid angles [4]:

$$\Omega_{s2-3496} = \Omega_{s2-7531} - \Omega_{s2-7621} - \Omega_{s2-8431} + \Omega_{s2-8921}$$

#### 2. Optical photon attenuation within crystal

Denote  $u$  as the attenuation length within a crystal, which means a beam of optical photons travel a distance of  $u$  and attenuates to  $1/e$  of its original intensity. In LYSO crystal, considering absorption and Rayleigh scattering,  $u$  is set to 121mm [3].

#### 3. Multiple specular reflection

Optical photons are reflected or refracted in crystal surface. Refracted photons are then reflected or absorbed by reflecting film. Probability that a photon reaches a certain SiPM pixel after  $n$  times of reflection, is determined as follow:

$$p = \sum_{n=0}^{\infty} \left( \frac{d\Omega_n}{4\pi} \prod_{i=0}^n r_i \times \exp(-l_i / u) \right) \quad (2)$$

Where  $p$  is probability for a photon to be detected by a certain pixel,  $n$  is the number of reflections before a photon reaches a SiPM pixel.  $d\Omega_n$  is the solid angle within which a photon is emitted and reaches a certain pixel after  $n$  specular reflections,  $l_i$  is the distance from a mirror image source to center of a SiPM pixel, and  $r_i$  is the reflectivity for  $i$ th specular reflection.

3.1)  $d\Omega_n$  is calculated using mirror image method. Fig 3.a shows, photons emitted from S1 can reach a certain pixel at M1, only if they are emitted within a certain solid angle. This solid angle equals to the angle the pixel subtends as seen from S2, the mirror image of S1 about M2.  $d\Omega_n$  is calculated by formula (1). As Fig 3.b shows, sum up the probability for different reflection number  $n$ , we can get the final result. Fig3.b only shows 1D circumstance, in simulation we consider virtual iamges in 3D space, then

$$p = \sum_{nz=0}^{\infty} \sum_{ny=0}^{\infty} \sum_{nx=0}^{\infty} \left( \frac{d\Omega}{4\pi} \prod_{i=0}^{nx} r_i \prod_{j=0}^{ny} r_j \prod_{k=0}^{nz} r_k \times \exp(-l_{i,j,k} / u) \right) \quad (3)$$

$r_i$ ,  $r_j$  and  $r_k$  represents reflectivity in  $x$ ,  $y$  and  $z$  direction.

Testing result shows the sequence of (2) converges quickly, so we set upper bound of  $nx$ ,  $ny$  and  $nz$  as 20, which ensures enough accuracy.

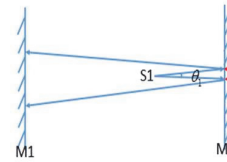


Fig3 a. S2 is the mirror image of S1 about M2,  $\theta_1 = \theta_2$

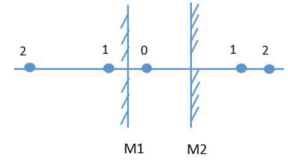


Fig 3.b, mirror images, the numbers are  $n$  in formula (2)

3.2) We will prove  $r_i$  is the same for different  $i$  in formula (2), for a given  $(nx, ny, nz)$  in a specular cuboid detector. Denote vector  $(v_x, v_y, v_z)$  as the propagation direction of a light beam, in a specular cuboid detector, after reflection only one element changes into its opposite number, let it be  $(v_x, v_y, -v_z)$ . Normal vectors of a surface are  $(1, 0, 0)$ ,  $(0, 1, 0)$  and  $(0, 0, 1)$ . Before and after reflection, the angle between direction vector and surface normal vectors remains the same. For a fixed incidence angle, reflectivity  $r$  is determined by Fresnel's law. Suppose a virtual image of point source is located at  $(x_l, y_l, z_l)$ , for a pixel with its center located at  $(x_p, y_p, 0)$ , we can calculate angle between light beam travelling direction  $(x_p - x_l, y_p - y_l, -z_l)$  and normal vector  $(1, 0, 0)$ , denote it as  $\theta_i$ . Then

$$r_x = \frac{1}{2} \left[ \left( \frac{n_1 \cos \theta_i - n_2 \cos \theta_t}{n_1 \cos \theta_i + n_2 \cos \theta_t} \right)^2 + \left( \frac{n_1 \cos \theta_i - n_2 \cos \theta_t}{n_1 \cos \theta_i + n_2 \cos \theta_t} \right)^2 \right] \quad (4)$$

Where  $n_1$  is refraction index of crystal,  $n_2$  is refraction index of silicone grease.  $\theta_i$  is optical photon incident angle and  $\theta_t$  is the exit angle. Then formula (3) can be written as

$$p_i = \sum_{nz=0}^N \sum_{ny=0}^N \sum_{nx=0}^N \left( \frac{d\Omega_{nx,ny,nz}}{4\pi} r_x^{nx} r_y^{ny} r_z^{nz} \times \exp(-l_{nx,ny,nz}/u) \right) \quad (5)$$

$p_i$  is the probability a photon is detected by SiPM pixel  $i$ .  $N$  is a constant upper bound of total reflection number. Definition of other variables are the same as formula (2).

This analytical model is generic. For different film types, only reflectivity is different, which will be shown in following part. Considering optical photon transportation between bottom surface and SiPM, each item in formula (5) needs to multiply  $p_{z,bottom}$ , and  $p_{z,bottom}$  is the probability an optical photon travel through silicone into SiPM, depending on the optical design of the detector.

#### 4. BS model

Optical photon transportation can has several stages: some photons are emitted towards bottom surface and get detected, probability of this process is determined by solid angle a SiPM pixel subtends seen from the point source; other photons are emitted towards other surfaces and then get reflected or refracted; refracted photons are absorbed by black film, and reflected photons will go back into crystal. Light distribution is determined by formula (4) and (5).

#### 5. SS model

In SS model, the reflectivity at a crystal surface composes of two parts, direct reflection (Y1) and refraction-reflection (Y2, Y3 and Y4).

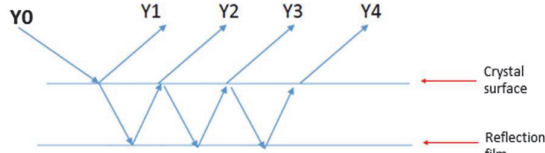


Fig 4, Optical photon transportation between crystal surface and reflection film

For a specular film, intensity of light beam Y1, Y2, Y3... is a geometric sequence, where  $Y1/Y2=pq$ ,  $p$  is reflectivity from silicone to crystal, and  $q$  is reflectivity in reflection film.  $r_x$  is calculated from formula (4), and  $r$  in formula (5) is

$$r = r_x + (1 - r_x) \times [pq + (pq)^2 + (pq)^3 + (pq)^4 + (pq)^5] \times (1 - p) / p \quad (6)$$

5 items are selected to simplify calculation without degrading accuracy.

#### 6. DS model

Ideal diffuse film obeys Lambert's cosine law, the luminous intensity is directly proportional to the cosine of the angle between direction of incident light and surface normal [5].

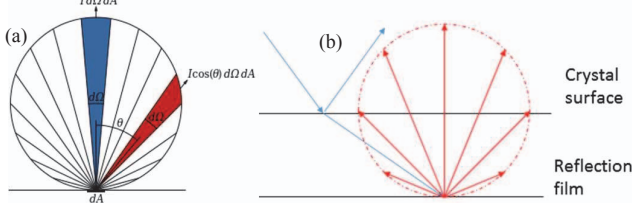


Fig 5. (a) Lambert's cosine law (b) Optical photon transportation between crystal surface and ideal diffuse film

Optical photons reaching crystal surface are reflected or refracted. Refracted photons then go through Lambertian reflection as shown in Fig 4.b. So the total reflectivity can be written as

$$r = r_x + (1 - r_x) \frac{d\omega d\theta}{\pi} \left( \int_0^{\pi/2} \int_0^{2\pi} \cos \theta \sin \theta d\theta d\varphi = \pi \right) \quad (7)$$

$r_x$  is calculated by (4),  $\theta$  is the incident angle.  $d\omega$  is the solid angle of a SiPM pixel seen from a virtual image,  $d\omega$  changes with  $\theta$  but is set to a constant because it's usually small.

Only optical photons that behave as if they are reflected from a specular film are counted. Other diffuse photons contribute to a constant background. This background is determined by the assumption that, total counts of detected photons are the same for SS and DS model when photon absorption probability of film is the same.

#### C. Monte Carlo Simulation

GATE Monte Carl simulation was performed to evaluate this model. The size of the scintillator was  $20 \times 20 \times 20 \text{ mm}^3$ . An isotropic optical point light source was placed at certain typical positions within the scintillator, and photons were collected by the detector. Number of optical photons collected by each SiPM pixel was extracted from simulation data. To control statistical error, in each simulation total number of photons was above 1 billion.

#### D. Definition of CC and NMSE

Two factors were defined to measure difference between light distribution obtained from simulation and model calculation. Denote the light spread matrix of simulation as  $\{a_i\}$ , and light spread of model calculation as  $\{b_i\}$ , where  $a_i$  and  $b_i$  are number of photons collected by SiPM pixel  $i$ . Correlation coefficient (CC) and normalized mean square error (NMSE) are defined as follow

$$CC = \sum_i a_i b_i / \left( \sqrt{\sum_i a_i^2} \sqrt{\sum_i b_i^2} \right) \quad NMSE = \sqrt{\sum_i (a_i - b_i)^2} / \sqrt{\sum_i a_i^2}$$

CC measures similarity in shape of light distribution, and MSE measures difference in amplitude of light distribution.

### III. RESULTS

Size of detector is  $20 \times 20 \times 20 \text{ mm}^3$ , coordinates are as shown in Fig1. For every treatment of film, point source is put at five positions, CC and MSE are calculated for each simulation.

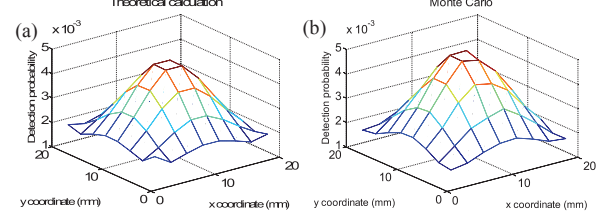


Fig 6. light distribution calculated from (a) analytical model (b) simulation

Fig 6 shows results of analytical model and simulation. Optical point source is positioned at center of block, surface treatment is SS (polished crystal surface, specular film). Center part is close to source, and has higher counts. Full result is shown in Table 2. The result shows that this solid-angle based model is very accurate, with CC above 0.99, and MSE below 0.13.

Table2. Results of light distribution model and Monte Carlo simulation

Position of point source	BS Model		SS Model		DS Model	
	CC	NMSE	CC	NMSE	CC	NMSE
(10,10,2)mm	0.9998	0.0076	0.9999	0.0342	0.9992	0.0611
(10,10,10)mm	0.9992	0.0662	0.9999	0.1143	0.9996	0.0419
(10,10,19)mm	0.9999	0.0887	0.9998	0.1226	0.9997	0.0304
(10,19,10)mm	0.9999	0.0823	0.9999	0.1058	0.9988	0.0698
(17,18,19)mm	0.9999	0.1111	0.9998	0.1215	0.9965	0.1217

### IV. SUMMARY

In this paper, an analytical model to characterize optical photon transportation in monolithic PET detector is proposed. The general idea is to calculate the detection probability of optical photon emitted at a given position. The probability was calculated as the solid angle subtended by the detector pixel seen from a certain source position, and mirror image method was used to deal with multiple reflections. Crystal surface treatments with three types of commonly used reflecting film were considered.

Accuracy of the proposed model was validated using GATE Monte Carlo simulation. For each surface treatment case, a point source is put at 5 different positions, and the light distribution at bottom surface is compared with result of this model. Excellent agreement was observed between calculated and simulated light distributions for all cases, indicating the accuracy of the model. This model can potentially facilitate positioning algorithm design for monolithic PET detectors. It is also useful to provide guidance in design of monolithic scintillator detector. Further refinements of the model includes adding optical transportation process in coupling layer between the crystal and SiPM, and considering electrical noise.

### REFERENCES

- [1] Lewellen, Tom K. "Recent developments in PET detector technology." *Physics in medicine and biology* 53.17 (2008): R287.
- [2] Barrett, Harrison H., et al. "Maximum-likelihood methods for processing signals from gamma-ray detectors." *Nuclear Science, IEEE Transactions on* 56.3 (2009): 725-735.
- [3] DJ, van der Laan, et al. "Optical simulation of monolithic scintillator detectors using GATE/GEANT4." *Physics in Medicine & Biology* volume 55.6(2010):1659-1675(17)
- [4] Gotoh, H., and H. Yagi. "Solid angle subtended by a rectangular slit." *Nuclear Instruments and Methods* 96.3 (1971): 485-486.
- [5] Oren, Michael, and Shree K. Nayar. "Generalization of Lambert's reflectance model." *Proceedings of the 21st annual conference on Computer graphics and interactive techniques*. ACM, 1994.